Three dimensional numerical lining damage analysis under pore pressures

Saba GHAREHDASH, Amirkabir University of Technology, Iran, milisaba.46@hotmail.com
Milad BARZEGAR, Amirkabir University of Technology, Iran, milisaba.46@gmail.com
Mostafa SHARIFZADEH, Curtin University, Western Australia, m.sharifzadeh@curtin.edu.au

Topic (Planning and Designing Tunnels and Underground Structures)

In this study, the behavior of lining subjected to pore pressure is investigated using three dimensional finite difference numerical modeling. In the analyses, Mohr-Coulomb failure criterion has been used for the characterization of the lining strength. Stresses acting on the lining boundary have been simulated by an exponential function which reaches its maximum within a long time and then falls to zero value in a considerable period. The strain rate effect on the mechanical properties of lining has also been taken into account in the analyses. Different lining conditions have been studied to investigate the effects of pore pressure rate and anisotropic high in situ stresses on lining performance and pore pressures induced damage zones. Results have shown that the most efficient support in lining will be the one with low water content but with a sufficiently high confinement pressure. In addition, it has been verified that the directions and the magnitudes of major principle stresses affect the development of the damage zone around the lining. Finally, it has been seen that proposed equation for the pore pressure of soil material fits very well to general suggestions.

Keywords: *Lining, Pore Pressures, Numerical Modelling, Principal Stresses*

1. Introduction

Segment is the basic structure unit of a shield tunnel. Lining is the main part of the segment. The mechanical behavior of the lining affects the form of reinforcement, the ratio of reinforcement and the cost of whole tunnel. Therefore, it is significant to clarify the mechanical behavior of lining in construction stage under pore pressures, which can save the engineering investment and optimize the segment design. Foregoing researches (Blom et al., 1999; Nomoto et al., 1999; Sramoon and Sugimoto, 2002 Koyama, 2003; Kasper and Meschke, 2004) seldom involve the mechanical behavior of segment lining. At present, the methods of research on segment lining are mostly limited in the indoor full size experiments plus some field measurements. Zhang et al. (2002) tested the lining stress of segment joints through indoor experiments. Chen et al. (2004) performed a field measurement on one section of shield tunnel in Guangzhou Metro and researched the property of lining in different work conditions. Dobashi et al. (2004) researched the rational design of steel segmental lining in Central Circular Route. Due to the various types of loads and the complicated boundary conditions, it is very difficult to simulate the actual loads and boundary conditions in indoor experiment. If the loads and boundary conditions are not precisely simulated, the lining stress measured indoors may have rather large errors. Field measurement may be quite precise for lining stress. However, for different tunnels, the limited test results cannot reflect the whole picture of their lining's mechanical behavior under different construction and geological conditions.
In this paper, a load-structure theory was applied. A finite element (FE) program of ADINA was adopted to establish a 3D numerical model for the shield tunnel. In order to simulate the actual situation precisely, key segment and tail of shield machine were considered. The lining stresses in the normal construction stage and under pore pressures were analyzed.

2. 3D finite element model

The three dimensional model was developed for the project using the finite element package. The finite element model has been created to replicate the tunnel lining. The particular features of the model are described below see Fig. 1. Each segment has been modelled as a discrete structure comprised of a grid of quadrilateral plate elements. The geometry of these segments incorporates a taper of 100 degrees along longitudinal joints. At the interface between adjacent segments, rigid links and contact elements have been used to model the action of joints permitted to pivot about the inner or outer edges of the joint bearing surface. The rigid links along each joint face extend perpendicular to the plate elements to either edge of the bearing surface. The links have been connected with compression-only springs to allow separation to occur and so allow joint rotation. Each compete ring consists of 2400 nodes, 287 beams, 1800 plates and 384 links elements (Fig. 2).

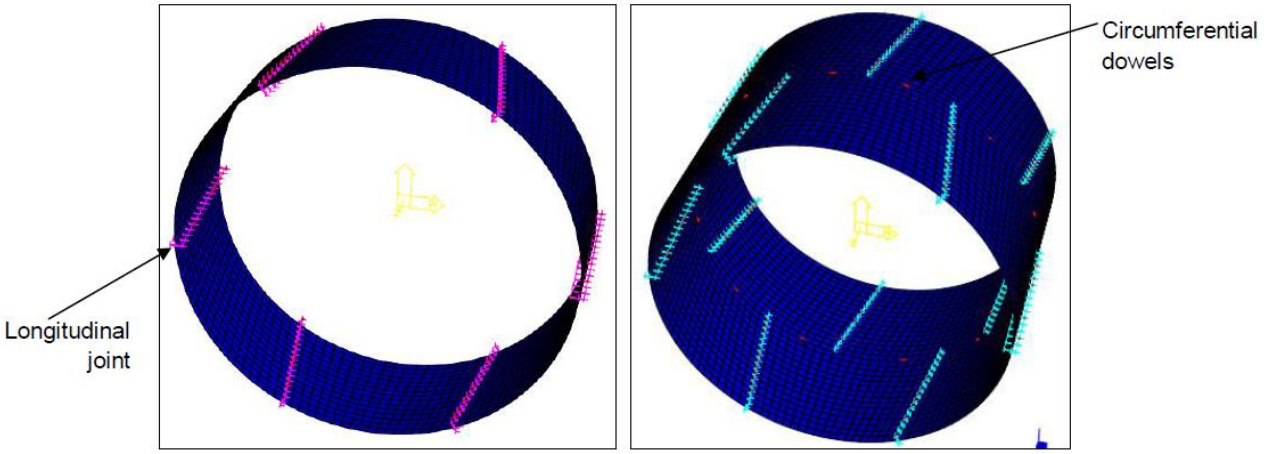

Fig. 1 *(a) 3D model of tunnel ring with tapered longitudinal joints (b) 3D coupled model*

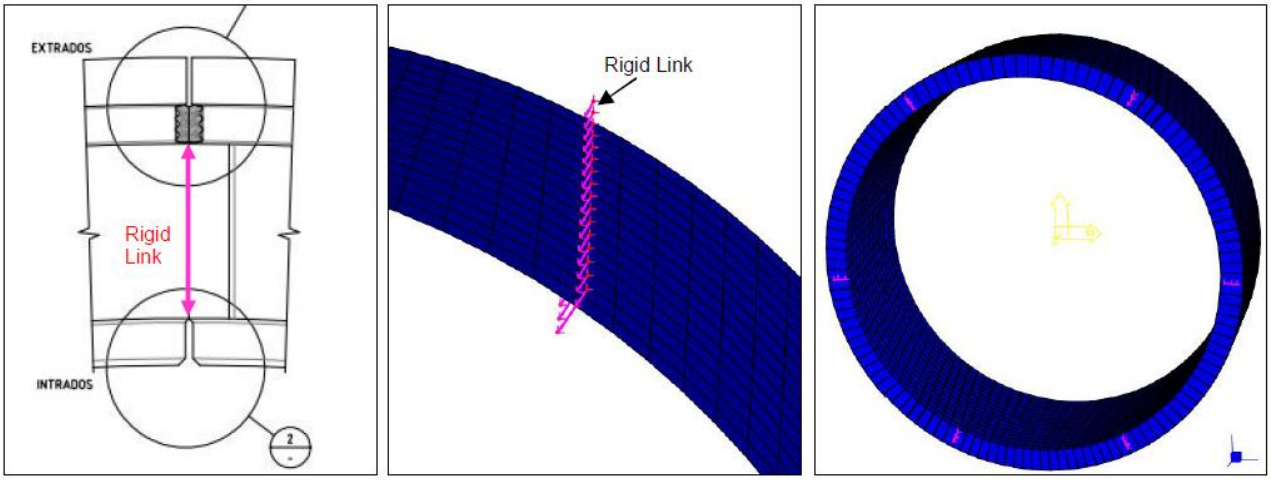

Fig. 2 *(a) Longitudinal joint (b) Rigid link used to model tapered joint (3) 3D solid model showing joint behavior*

Suppose the surface of the liner is completely permeable and consequently, the pore pressure at the surface vanish, then according to (1), the following relation can be obtained

$$b_n = (- A_f K^2_f H^2_n (k_f R)/A_s k_s^2 H_n^2 (k_s R))a_n - ((-i)^n A_f k_f^2 A_{p1}^{(l)} J_n(k_f R))/A_s k_s^2 H_n^2 k_s R), \quad -\infty<n<+\infty \qquad (1)$$

The linear equations for the unknown coefficients b_n, a_n can be obtained using Biot's theory.

2.1 Response of a liner with six pieces and six joints subjected to pore pressures

Here the pore pressures of a tunnel lining with six liner pieces and six joints will be calculated as a numerical modelling. The porous medium in this has the same parameters described in equation 1. The radius of the liner R = 6.0m. The thickness and the width of liner are h = 0.3m, b =1.0m, respectively. Young's modulus and Possion's ratio of the liner material are $E = 3.5\times10^{10}$ Pa and υ= 0.3, respectively. The density of the tunnel liner is $\rho = 2.0\times10^{3}$ kg/m^3. The central open angles for the six joints are equal to 3^0, respectively, while the central open angles for the six liner pieces are equal to 57^0, respectively. Moreover, the middle points of the six joints are located at 00, 600, 1200, 1800, 2400 and 3000, respectively. Fig. 3 also demonstrates that the difference of the bending moment between the two cases becomes obvious especially around the joints. Moreover, the responses of the liner segments at the incident side is larger than that of shelter side. The difference of the bending moment between the two cases becomes more obvious for the pore pressures: in regions near the joints, the piecewise liner is subject to much larger internal force (Q, M) than the homogeneous liner.

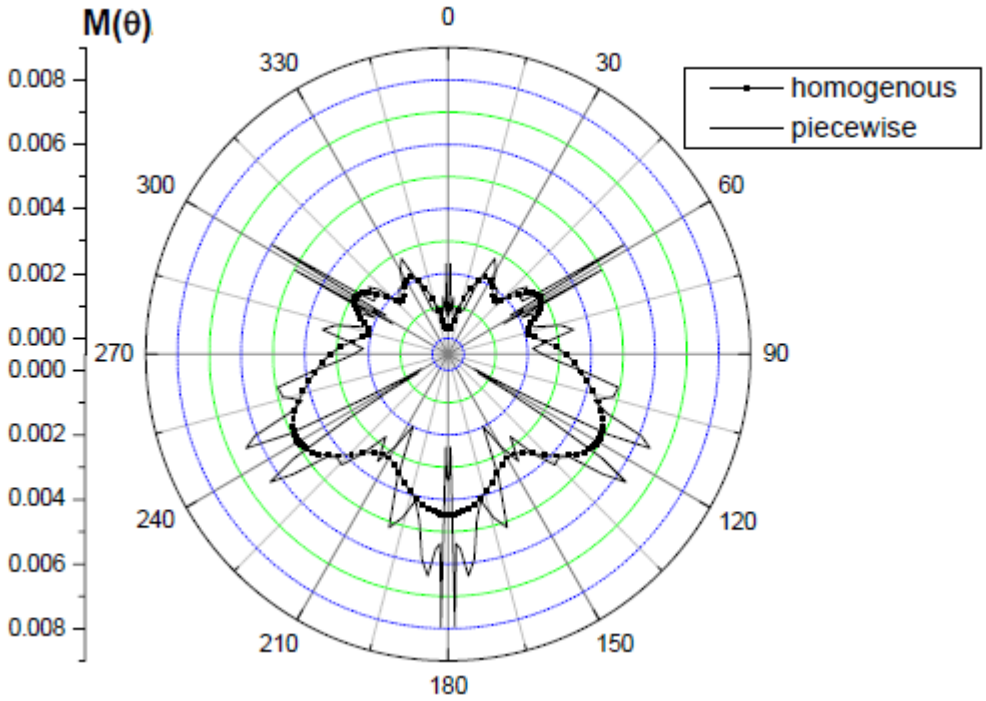

Fig. 3 *Response of bending moment a homogeneous and a piecewise tunnel liner with six liner pieces and six joints and subject to pore pressures*

As showed in Figs. 4 and 5, under different pore pressures, squeezing action of lining causes apparently irregular displacement. The position of maximum displacement is also irregular. In order to clarify the irregular displacement state, displacement is showed in side view (Fig. 5). The red dash lines denote initial position of segments. The deformation mesh of tunnel indicates the entire displacement tendency is bending about horizontal axis. But for one segment, the displacement is irregular (Figs. 4–5).

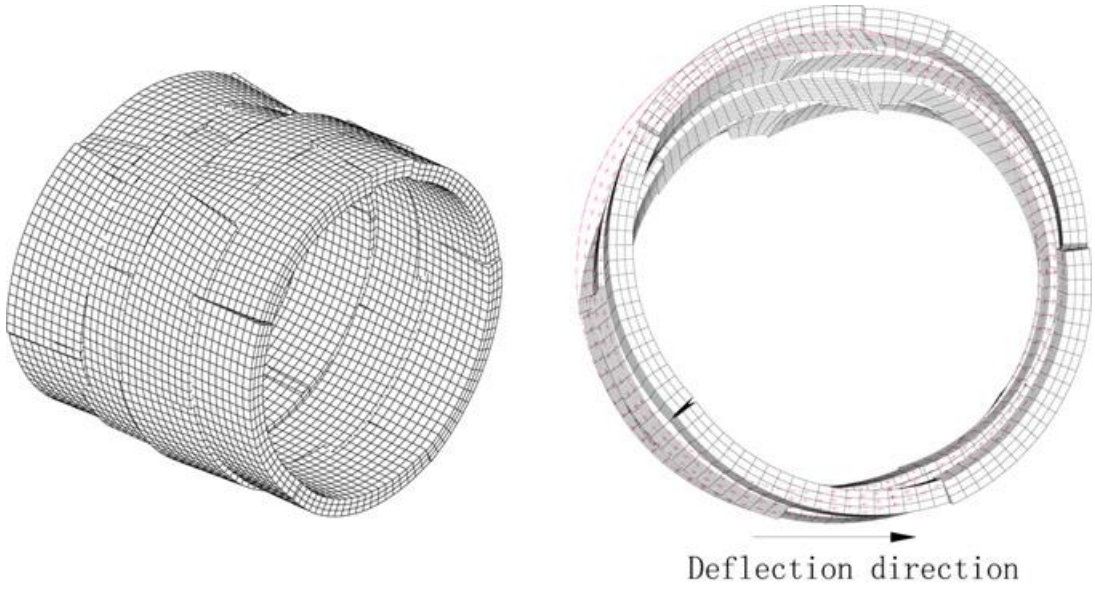

(a)

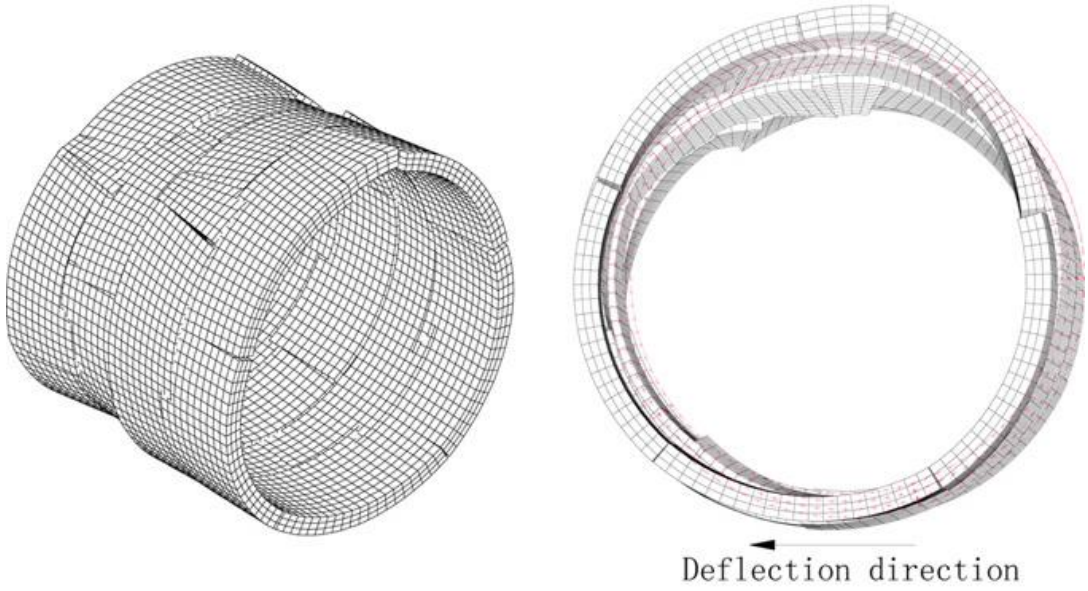

(b)

Fig. 4 *Displacement of ring with different pore pressures*

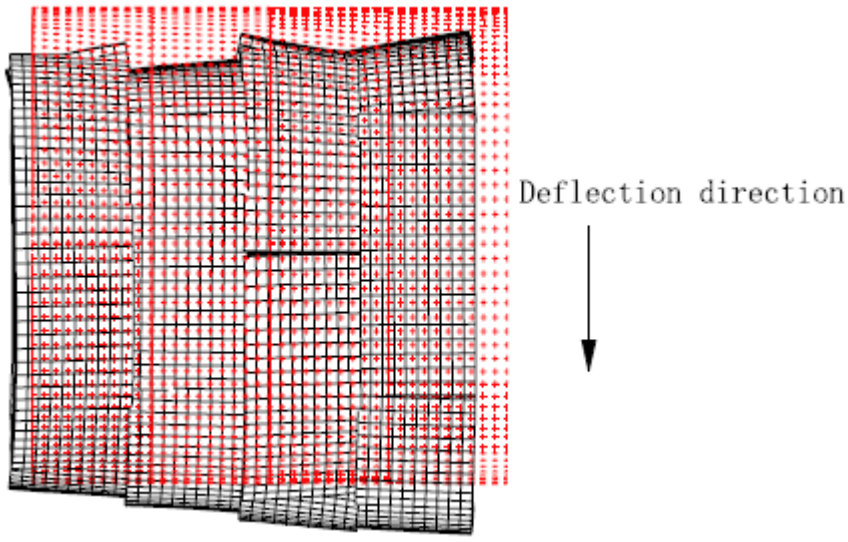

Fig. 5 Displacement of ring (side view)

2.2 Stress distribution

It is obvious that stress concentration area is the same as maximum dislocation area. Fig. 6 indicates the maximum dislocation appears in lining with joint, therefore, the following figures just shows the first principal stress in lining. Fig. 7 indicates that stress concentrates near bolt hole of key segment. Result of pore pressure attitude without deflection is showed in Fig. 6. Compare Fig. 6 with Fig. 7, stress distribution in Fig. 6 is more intensive than that in Fig. 7, and the stress peak values in models with deflection are much larger than that in model without deflection. However, there are some loading combinations where the pressure exerted by groundwater has an overall adverse impact, such as when considering high axial loading in combination with the structural effects of tunnel non-circularity (as caused by build tolerances and non-uniform loading) For these cases the design hydrostatic pressure was considered and applied to the three dimensional model developed for the project. The premise for applying full groundwater pressures is that there will be full hydraulic connectivity through the rock mass, such that water can migrate through geological discontinuities (e.g. jointing and faults) in the rock mass.

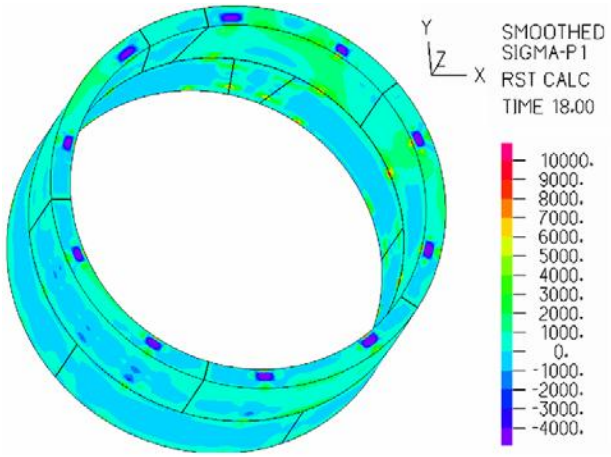

Fig. 6 *σ_1 Contour in lining with pore pressure (kN/m^2)*

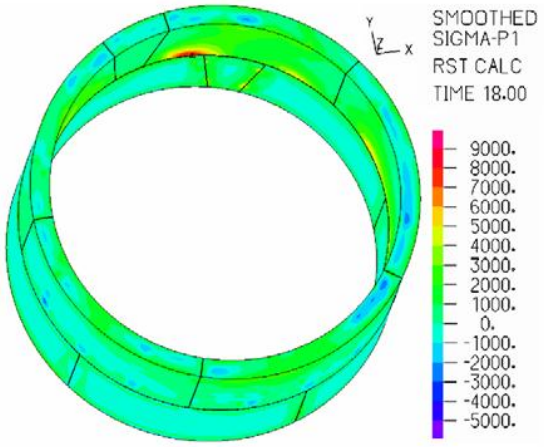

Fig. 7 *σ_1 Contour in lining without pore pressure (kN/m^2)*

Looking at Fig. 8 at 1 and 2MPa pore pressure loading the lining displacement pattern is fairly similar, but by increasing the loading to 4MPa the rockmass displacement changes in a more gradual manner.It is visible that as the loading increases, a significant displacement occurs in the lining all along the area. To further illustrate the effect of lining displacement on pore pressure behavior, the lining stresses are shown in the three simulated cases in Fig. 9.

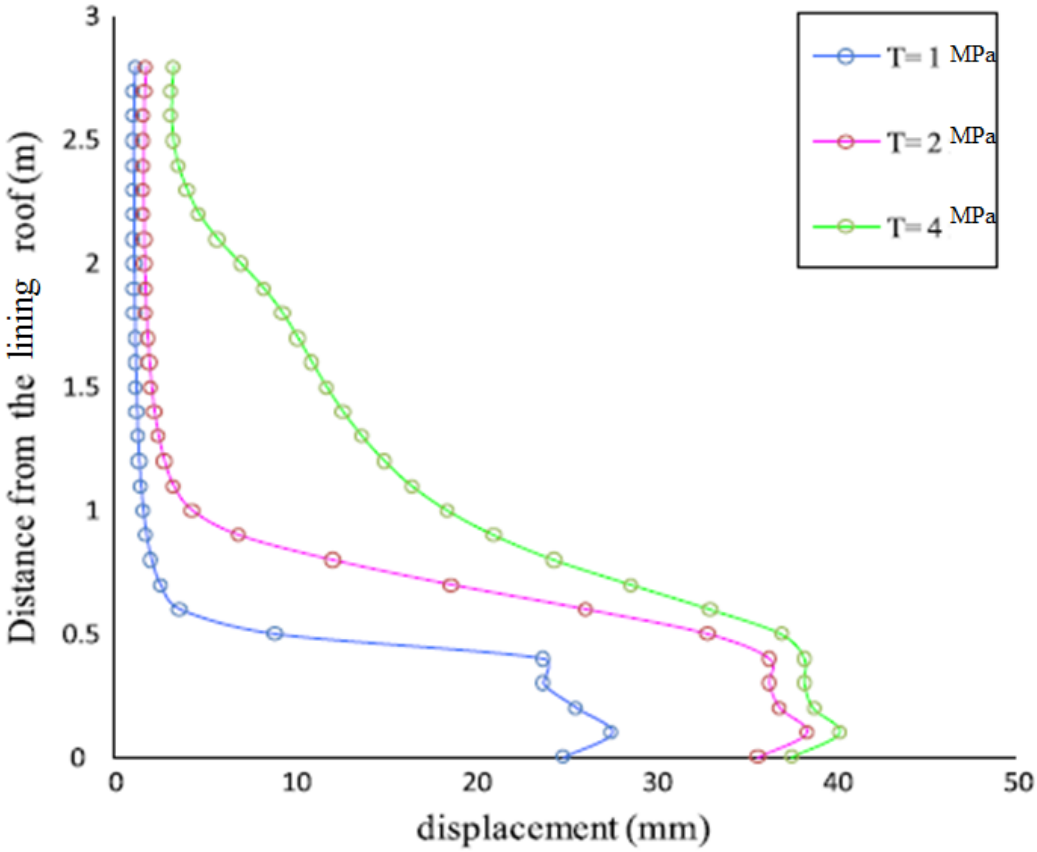

Fig. 8 *Change in lining displacement around the rockmass for various pore pressure loadings.*

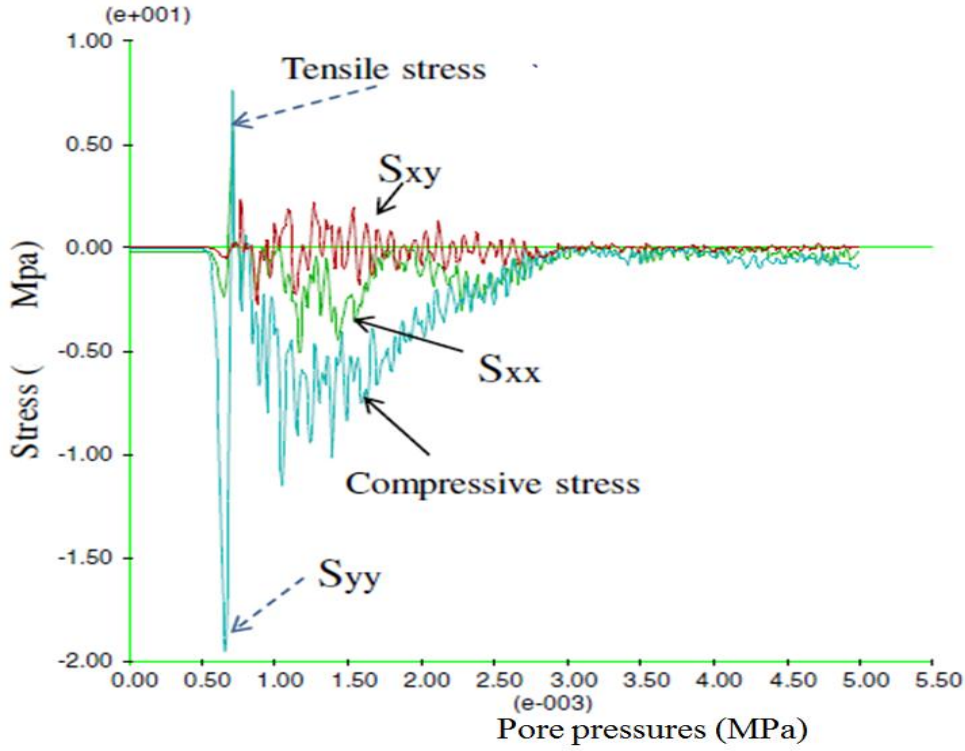

Fig. 9 *Change in lining stresses around the rockmass for various pore pressure loadings.*

Fig. 9 shows the variation of S_{xx}, S_{yy}, and S_{xy} at the lining nodes. As can be seen from Fig. 9, the maximum magnitude of the S_{yy} stress is about 19.5MPa, while the maximum values of S_{xx} and S_{xy} are approximately 5 and 2.5MPa, respectively. Therefore, lining fracturing in the zones close to the

roof is due to high S_{yy} stress. Moreover, maximum tensile stress is about 7.6MPa which is due to pore pressure loadings.

3. Conclusion

Through analyzing of a 3D numerical model of lining tunnel with 9 rings, some conclusions are drawn as follows:
(1) In normal construction status, the joint of segment is in elastic status and its stress is between −65MPa and 20MPa.
(2) When applying pore pressures, the stress of segment lining is between −80MPa and 50MPa, and the lining is not in elastic status. Lining attitude of shield machine has effect on principal stresses distribution and peak value. Comparison of the S_{yy} stress before and after the pore pressures loading shows that the stress increment after applying pore pressures is between 0 and 20MPa. In general, the lining is in plastic status.
(3) The stress of segment lining is at a low level, which accords with actual measurement. Even as some cracks appear on segments, the stress of segment is still at a low level. That is to say, the segment cannot protect the plain concrete covering layer of segment. Certain impact force or tension stress causes the crack of the thick plain concrete covering layer. It is helpful to incorporate a certain quantity of steel fiber to improve the anti-crack and shock resistance performance.

4. References

ADINA R&D Inc., 2005. Theory and Modeling Guide Volume I: ADINA Solids & Structures. Watertown, MA.

Blom, C.B.M., Horst, E.J.V., Jovanovic, P.S., 1999. Three-dimensional structural analyses of the shield-driven "Green Heart" tunnel of the high-speed line south. Tunnelling and Underground Space Technology, 14(2):217-224. [doi:10.1016/S0886-7798(99)00035-8].

Chen, W., Peng, Z.B., Tang, M.X., 2004. Testing study on working property of shield segment. Chinese Journal of Rock Mechanics and Engineering, 23(6):959-963 (in Chinese).

Dobashi, H., Kawada, N., Shiratori, A., 2004. A rational design of steel segmental lining in large dimensional shield tunnels for rapid post-excavation method. Tunnelling and Underground Space Technology, 19(4-5):457-458. [doi:10.1016/j.tust.2004.02.065]

Kasper, T., Meschke, G., 2004. A 3D finite element simulation model for TBM tunnelling in soft ground. International Journal for Numerical and Analytical Methods in Geomechanics, 28(14):1441-1460. [doi:10.1002/nag.395]

Koyama, Y., 2003. Present status and technology of shield tunneling method in Japan. Tunnelling and Underground Space Technology, 18(2-3):145-149. [doi:10.1016/S0886-7798(03)00040-3]

Li, H.P., An, H.W., Xia, M.Y., 2006. Analysis of dynamic character of tunneling shield machine. Chinese Journal of Underground Space and Engineering, 2(1):101-103 (inChinese).

Li, Z.N., 2001. Discussion on Manufacture Tolerance of Shield Tunnel Segment. Papers of 14th Meeting of Council of Fast Track Communication of China Civil Engineering Society, Beijing, p.308-312 (in Chinese).

Li, Z.N., Chen, L.N., 2003. Discussion on Form of Reinforcement in Segment of Shield Tunnel. Papers of 15th Meeting of Council of Fast Track Communication of China Civil Engineering Society, Chengdu, p.73-75 (inChinese).

Mashimo, H., Ishimura, T., 2003. Evaluation of the load on shield tunnel lining in gravel. Tunnelling and Underground Space Technology, 18(2-3):233-241.[doi:10.1016/S0886-7798(03)00032-4]

Nomoto, T., Imamura, S., Hagiwara, T., Kusakabe, O., Fujii, N., 1999. Shield tunnel construction in centrifuge. Journal of Geotechnical and Geoenvironmental Engineering, 125(4):289-300. [doi:10.1061/(ASCE)1090-0241(1999) 125:4(289)]

Qin, J.S., Zhu, W., Chen, J., 2004. Study of dislocation of duct pieces and crack problems caused by shield attitude control. Construction Technology, 33(10):25-27 (in Chinese).

Sramoon, A., Sugimoto, M., 2002. Theoritical model of shield behavior during excavation. Journal of Geotechnical and Geoenviormental Engineering, (2):138-165.

Terzaghi, K., Peck, R., Mesri, G., 1996. Soil Mechanics in Engineering Practice. John Wiley and Sons, New York, p.104-105. Working Group No.2, International Tunneling Association, 2000. Guidelines for the design of shield tunnel lining. Tunnelling and Underground Space Technology, 15(3):303-331. [doi:10.1016/S0886-7798(00)00058-4]

Zhang, H.B., Yin, Z.Z., Zhu, J.G., Li, C.X., 2005. Three-dimensional FEM simulation of shield drivern tunneling during construction stage. Rock and Soil Mechanics, 26(6):990-994 (in Chinese).

Zhang, H.M., Guo, C., Fu, D.M., 2002. Study on load test of segment joint in shield driven tunnel. Modern Tunnelling Technology, 39(6):28-33 (in Chinese).

Zhu, W.B, Ju, S.J., 2003. Causes and countermeasures for segment cracking in shield-drivern tunnel. Modern Tunnelling Technology, 40(1):21-25 (in Chinese).